Multi-Atlas Segmentation of the Prostate: A Zooming Process with Robust Registration and Atlas Selection

Yangming Ou, Jimit Doshi, Guray Erus, and Christos Davatzikos

Section of Biomedical Image Analysis (SBIA)
Department of Radiology, University of Pennsylvania

Abstract. As an entry to the MICCAI 2012 Prostate Segmentation Challenge, this paper presents a multi-atlas-based automatic pipeline for segmenting prostate in MR images. Image registration is needed to transfer expert-defined ground-truth prostate segmentation from atlases onto target image. However, registration is rendered difficult in this dataset, due to different images having different field of view (FOV), different imaging protocol (from multiple imaging centers), large anatomical variability around prostate and large pathologic variability (some having enlarged prostate or prostate cancer). To overcome these limitations, we propose a "zooming process" for multi-atlas-based prostate segmentation. We first register all atlases onto target image to obtain an initial segmentation of the prostate. This step includes robust registration, atlas selection and majority-based label fusion. Then, we "zoom-in": re-run all atlas-to-target registrations, but this time restricting the registration to the vicinity of the prostate, ignoring compounding structures that are far away from the prostate and are largely variable. As a result, we can expect more accurate registrations and hence refined prostate segmentation. Our cross-validated results show improvement in segmentation by robust registration and atlas selection, compared to using all atlases. Additional improvement is observed when zooming in and focusing on registration of the prostate vicinity. We report average 0.84 dice overlap with expert-defined prostate segmentation in training subjects. Accuracy in testing datasets will be released by organizers of this challenge.

1 Introduction

In MICCAI 2012 Prostate Segmentation Challenge, participants are provided with 50 training prostate MR images, each having expert-defined prostate segmentation. The task is to segment prostate in 30 testing prostate MR images. In such a setting, we present a multi-atlas-based segmentation pipeline. The central idea is to transfer those expert-segmentations in training images (i.e., atlases) onto target image through image registration, and then fuse the transferred segmentations to derive an ultimate prostate segmentation in the target image. Previous studies (e.g., [1–4]) have reported plausible results using multi-atlas strategy to segment prostate, with average dice of 0.75–0.80 compared to expert-defined ground-truth.

In the dataset used in MICCAI 2012 Prostate Segmentation Challenge, several factors pose large difficulties to image registration, which is the fundamental component in multi-atlas segmentation framework. Those factors include: large variability of the MR images not only in terms of image intensity characteristics (e.g. scanner variability, inhomogeneities, etc.) but also in structures. Images may often have different field of views (FOVs) and are obtained from different imaging centers (see Fig. 3 for example). Consequently, the registration, affine or deformable, may often times fail. Aside from anatomical variabilities, this dataset contain some unidentified subjects with enlarged prostate or even prostate cancers, causing pathological variabilities.

To overcome these limitations, the proposed method is based on a zooming process: atlas-to-target registration to land an initial segmentation of prostate; then "zoom in", focusing only on the vicinity of prostate and re-do atlas-to-target registration to increase accuracy in registration and hence segmentation.

The key to guarantee the success of this zooming process is to obtain reasonably good initial segmentation of the prostate before zooming in to its vicinity. To this end, a registration method that is robust against the image variation is used, followed by iterative label fusion and atlas selection (it is not uncommon to expect certain number of registrations to fail, therefore we need to have an automatic mechanism to remove those failed cases from label fusion). Our experiments in training dataset will show that this strategy shall yield an initial segmentation of prostate that is of average 0.81 dice overlap with expert-segmentation (see Fig. 2 "phase 1" results). Obtaining this reasonably high accuracy is important, as we can now zoom in to the dilated version of the initial segmentation mask and expect the whole prostate being included in this dilated mask. The remaining part is straightforward – with much less interference from those structures far away from the prostate, we can focus on registering prostate vicinity well and finally obtained a refined final segmentation of the prostate. This zooming process has lifted the average dice to 0.84 in our experiment.

In the following, we will describe details of our pipeline in Section 2, with some demonstrations in training dataset in Section 3. Section 4 discusses and concludes this paper.

2 Methods

We will detail the proposed zooming process in this section. The whole pipeline is depicted in Fig. 1. In this figure, light pink box contains the first phase, where whole-image atlases are registered to whole-image target to land a tentative segmentation of the prostate (e.g., the orange region in the rightmost figure within pink box). Then, in the second phase, we zoom into prostate and its vicinity, as shown in the gray box. Here we refine all registrations and obtain the final segmentation of the prostate (e.g., the red region in the rightmost figure within gray box). The following two sub-sections will describe each of those two phases.

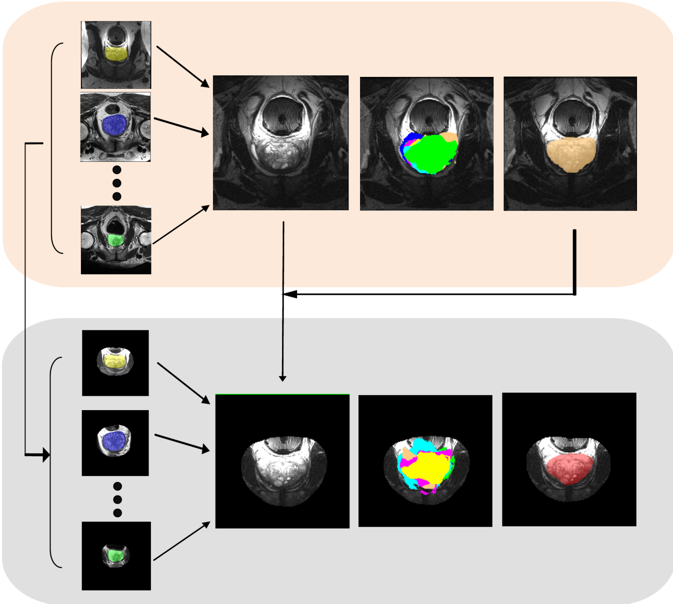

Fig. 1. The proposed pipeline. We rely on the whole atlases for initial segmentation of the prostate (phase 1, pink box), and then zoom in to the vicinity of prostate to obtain the final multi-atlas-based segmentation (phase 2, gray box).

2.1 Initial Multi-Atlas Segmentation: Find Prostate Location

In this first phase, we will use whole image registration from multiples atlases to target to obtain an initial segmentation of the prostate. Due to large variations in imaging protocols, FOVs, structures, anatomies and even pathology conditions among different subjects, registration from an atlas to the target is a very different task (see Fig. 3 for example). To ease this difficulty, we will describe below two measures: a) to use a robust registration algorithm; b) to automatically select atlases and potentially remove atlases whose registrations to target image have failed.

For registration algorithm, a recently-developed non-rigid registration algorithm is used for warping atlas images to the target. This algorithm, termed DRAMMS registration [5], is based on an attribute-based similarity metric. That is, it finds voxel correspondences by rich set of geometric texture at each voxel, other than by image intensity alone. The high dimensional multi-scale and multi-orientation Gabor textures have rendered each imaging voxel more distinctive and therefore better identifiable during search for correspondence. Furthermore, when registering an atlas to the target image, this algorithm relies more on the regions that can establish a more reliable matching compared to other regions. Such an approach is particularly well suited to the registration of prostate images, where the two images may have significant differences, or even missing correspondence (i.e., some structures present in one image but not the other).

For atlas selection and removal, we shall keep those atlases that are similar to target image and on the other hand, remove those atlases whose registrations to target image have failed. We automate this process in an iterative fashion. At the very beginning, we used all atlases for label fusion (using a population label fusion method STAPLE [6]). After having obtained a tentative prostate segmentation, we measure atlas-to-target similarity by a) mutual information (MI) within the tentative segmented region, b) correlation coefficient (CC) within the tentative segmented region and c) dice overlap between warped prostate region and the tentative prostate segmentation. Those atlases having less than 90% of the maximum MI, less than 90% of the maximum CC and less than 50% of the maximum dice overlap among all atlases are considered having failed registration with target image and thus removed. The remaining atlases are weighted by their $MI \times CC$ values in a globally weighted majority voting label fusion. The assumption here is to trust more on those atlases having higher similarity with the target image after registration. This way, we get an updated prostate segmentation. We iterate between label fusion and atlas selection/ranking until convergence. The convergence criterion is met if the prostate segmentations in two consecutive iterations become relatively stable ($>$ 90% dice), or otherwise repeat the above process till convergence. After convergence, the prostate segmentation mask in this phase 1 will be used for initializing phase 2 (focusing on prostate vicinity) in the next subsection. All the above mentioned parameters are optimized by leave-one-out experiments in training dataset.

2.2 Final Multi-Atlas Segmentation: Focus on Prostate Vicinity

The tentative prostate segmentation by the above phase 1 has an average 0.81 dice overlap with expert-define ground truth. This shows that phase 1 has successfully located majority part of the prostate in the target image.

With this reasonably good localization of the prostate in target image, we can now zoom in and focus on prostate vicinity in both atlas and target images. We first isotropically dilate the prostate mask obtained from phase to 1.5 times its volume, to make sure the dilated mask can cover the whole prostate (together with other surrounding structures). This way we have zoomed into prostate vicinity in the target image. To also zoom into prostate vicinity in atlases images, we proportionally dilate the ground-truth prostate masks in atlases. Readers can follow the arrows pointing from pink box to gray box in Fig. 1 to visualize this zooming process for extracting prostate vicinity in both atlases and target images. It should not be difficult to observe the immediate benefits of this zooming process – a large part of registration difficulties caused by different FOVs, different structures, and to some extent image inhomogeneity have been removed. Now we only need to register prostate vicinity in atlas and target images, which is a much easier problem than registering the whole images. Here we have also used DRAMMS registration software [5]. The resultant warped prostate masks are fused by the same strategy we have used in phase 1 (majority voting with iterative atlas ranking and selection).

3 Results

To demonstrate the effect of atlas ranking/selection and the effect of zooming process, we compared accuracies obtained from 4 different multi-atlas segmentation methods: MV – majority voting based on all warped atlases, no zooming process; STAPLE – based on all warped atlases, no zooming process; the proposed phase 1 – the proposed iterative weighted MV label fusion together with atlas ranking and selection, but no zooming process; the proposed phase 1+2 – the entire proposed pipeline, including both phase 1 (initial prostate localization) and phase 2 (zooming process with focus on prostate vicinity).

Fig. 3 visualizes segmentation by our proposed pipeline (green contours) as well as ground-truth segmentation (red contours), for 6 typical training subjects. These 6 subjects are randomly chosen from different imaging centers. For each subject, we used the remaining 49 subjects in training as atlases. During atlas selection, usually 10-15 atlases will be automatically kept. Fig. 2 quantifies segmentation accuracy in those cases, as measured by dice overlap with ground-truth segmentation.

We have several interesting findings from Fig. 2. First of all, atlas ranking and selection improve segmentation accuracy. This is expected, as removing those atlases that fail to register to target image should reduce confusions in label fusion. Also, the proposed zooming process does offer additional improvement in segmentation accuracy, accompanied by reduced standard error, showing the advantage of focusing on prostate vicinity.

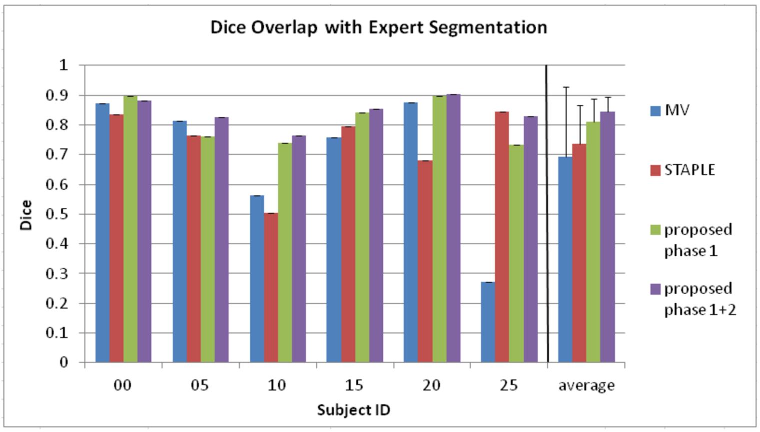

Fig. 2. Segmentation accuracy in 6 typical training subjects. Here accuracy is measured by dice overlap with expert-defined ground truth segmentation.

4 Discussion

This paper proposed a fully automatic pipeline for segmenting prostate MR images. We made two contributions in this study. The first is using robust image registration and especially atlas selection in multi-atlas-based segmentation framework. Due to large variability in prostate images across subjects, failure in atlas-to-target registration is not uncommon. Therefore, using robust image registration method to reduce the number of failures and developing criterion for removing failed atlases become key to accurate segmentation.

Our second contribution is the development of a zooming process and its proof of concept. The idea is to focus on registration of the prostate vicinity, in the hope of improving registration accuracy in prostate regions and hence the accuracy in segmentation. By doing so, we largely reduce the negative impact from those highly variable structures far away from the prostate. As a result, we observed significant improvement in segmentation accuracy.

We have applied this automatic pipeline to all 30 testing images in MICCAI 2012 Prostate Segmentation Challenge. Results will be disclosed by the organizers of this challenge.

References

1. Klein S, van der Heide UA, Lips IM, van Vulpen M, Staring M, Pluim JP., Automatic segmentation of the prostate in 3D MR images by atlas matching using localized mutual information. Med Phys. 35(4):1407-17 (2008).
2. Martin, S., Daanen, V., Troccaz, J., Atlas-based prostate segmentation using an hybrid registration. IJCARS, 3: 485–492, (2008).
3. Albert Gubern-Merida and Robert Marti, Atlas Based Segmentation of the prostate in MR images. MICCAI 2009 Prostate Segmentation Challenge.
4. Jason Dowling, Jurgen Fripp, Peter Greer, Sbastien Ourselin, Olivier Salvado, Automatic atlas-based segmentation of the prostate: A MICCAI 2009 Prostate Segmentation Challenge entry. MICCAI 2009 Prostate Segmentation Challenge.
5. Ou Y, Sotiras A, Paragios N, Davatzikos C, DRAMMS: Deformable registration via attribute matching and mutual-saliency weighting. MedIA 15(4):622-39, (2011).
6. Warfield SK, Zou KH, Wells WM, Simultaneous truth and performance level estimation (STAPLE): an algorithm for the validation of image segmentation, IEEE Trans Med Imag 23(7), 903-21 (2004).

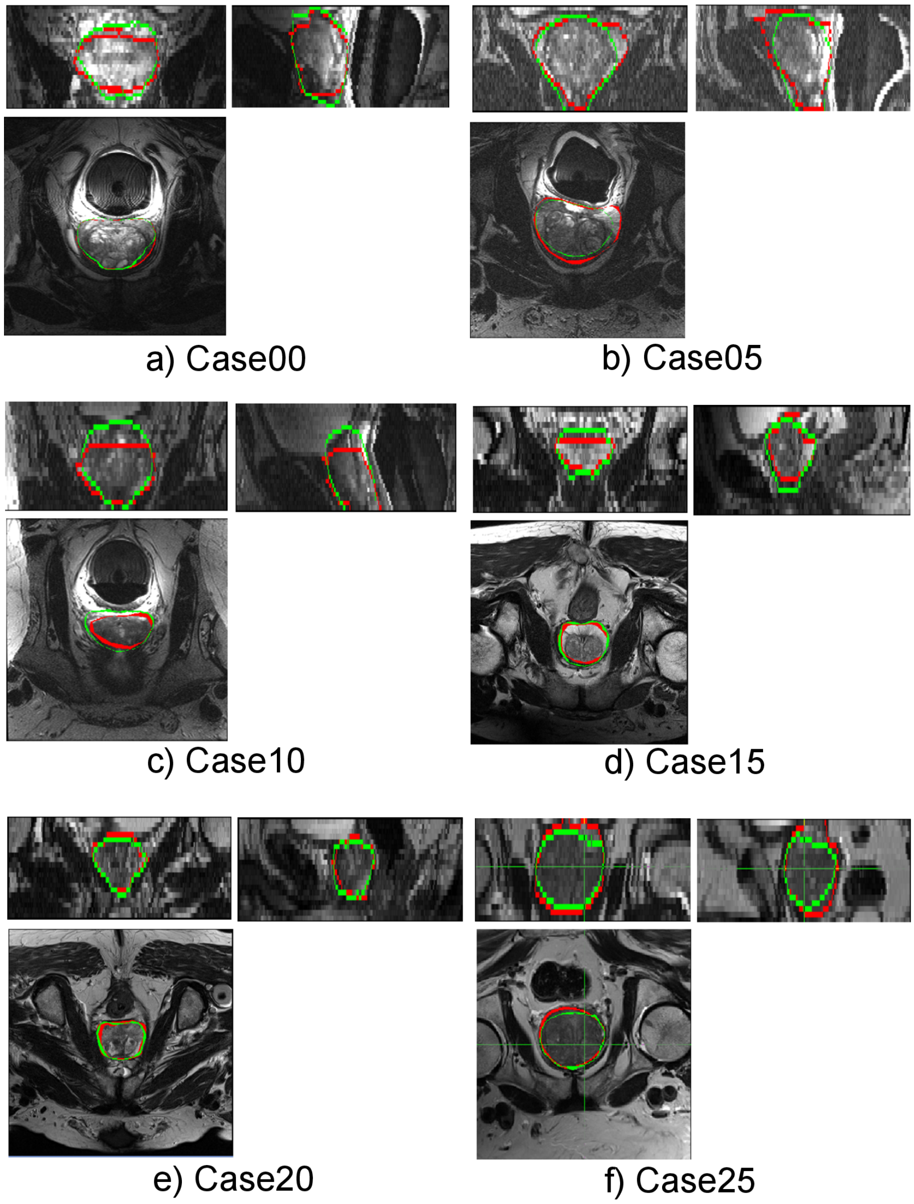

Fig. 3. Visualization of segmentation results in 6 randomly chosen subjects from training set. Red contours are ground truth by expert segmentation. Green contours are generated by our proposed pipeline.